

# Delayed Contrast Enhancement on MR Images of Myocardium: Past, Present, Future<sup>1</sup>

Karen G. Ordovas, MD  
Charles B. Higgins, MD

## Online CME

See [www.rsna.org/ry\\_cme.html](http://www.rsna.org/ry_cme.html)

### Learning Objectives:

- Describe the mechanism of delayed contrast enhancement of the myocardium.
- Describe the expected signal intensity of the infarct core, the peripheral zone, microvascular obstruction, and the remote myocardium on delayed-enhancement images after myocardial infarction.
- List the most common delayed-enhancement patterns seen in nonischemic cardiomyopathies.
- List two prognostic applications of myocardial delayed-enhancement images.

### Accreditation and Designation Statement

The RSNA is accredited by the Accreditation Council for Continuing Medical Education (ACCME) to provide continuing medical education for physicians. The RSNA designates this journal-based activity for a maximum of 1.0 *AMA PRA Category 1 Credit*<sup>™</sup>. Physicians should claim only the credit commensurate with the extent of their participation in the activity.

### Disclosure Statement

The ACCME requires that the RSNA, as an accredited provider of CME, obtain signed disclosure statements from the authors, editors, and reviewers for this activity. For this journal-based CME activity, author disclosures are listed at the end of this article. The editor and the reviewers indicated that they had no relevant relationships to disclose.

<sup>1</sup>From the Department of Radiology, UCSF Medical Center, 505 Parnassus Ave, Room L308, Box 0628, San Francisco, CA 94143-0628. Received October 14, 2009; revision requested November 17; revision received May 3, 2010; accepted May 14; final version accepted May 27. Final review by K.G.O. May 14, 2011. Address correspondence to C.B.H. (e-mail: [charles.higgins@radiology.ucsf.edu](mailto:charles.higgins@radiology.ucsf.edu)).

© RSNA, 2011

Differential enhancement of myocardial infarction was first recognized on computed tomographic (CT) images obtained with iodinated contrast material in the late 1970s. Gadolinium enhancement of myocardial infarction was initially reported for T1-weighted magnetic resonance (MR) imaging in 1984. The introduction of an inversion-recovery gradient-echo MR sequence for accentuation of the contrast between normal and necrotic myocardium was the impetus for widespread clinical use for demonstrating the extent of myocardial infarction. This sequence has been called delayed-enhancement MR and MR viability imaging. The physiologic basis for differential enhancement of myocardial necrosis is the greater distribution volume of injured myocardium compared with that of normal myocardium. It is now recognized that delayed enhancement occurs in both acute and chronic (scar) infarctions and in an array of other myocardial processes that cause myocardial necrosis, infiltration, or fibrosis. These include myocarditis, hypertrophic cardiomyopathy, amyloidosis, sarcoidosis, and other myocardial conditions. In several of these diseases, the presence and extent of delayed enhancement has prognostic implications. Future applications of delayed enhancement with development of MR imaging and CT techniques will be discussed.

© RSNA, 2011

**D**elayed gadolinium-enhanced magnetic resonance (MR) imaging of ischemic and nonischemic myocardial disease has become an important application of cardiovascular MR imaging during the past decade. At many sites where cardiac MR is performed, myocardial tissue characterization is one of the most frequent clinical indications. In this review we will discuss the development of the imaging techniques, physiologic mechanisms, clinical applications for diagnosis and prognosis, and future perspectives on the use of delayed-enhancement imaging.

### Essentials

- Both acute and chronic myocardial infarctions show delayed enhancement after administration of gadopentetate dimeglumine and other extracellular space gadolinium contrast media.
- Gadolinium-based contrast agents distribute in the extracellular space of normal myocardium and are excluded from normal myocardial cells but will distribute both extra- and intracellularly after loss of myocardial membrane integrity in the acute infarcted region.
- Recovery of contraction in regions with dysfunction after revascularization has been related to the transmural extent of delayed enhancement in patients with acute infarction and ischemic cardiomyopathy.
- Delayed-enhancement MR imaging can help identify and quantify a peripheral zone of myocardial infarction; patients with larger peripheral zones have increased risk for cardiovascular events, especially ventricular arrhythmias.
- Delayed-enhancement MR can demonstrate site of necrosis, fibrosis, and deposition of abnormal substrates in nonischemic myocardial diseases.

### Past: The Historical Perspective

While the clinical use of differential contrast enhancement of abnormal myocardium has been a relatively recent advance, the concept of differential enhancement of myocardial infarction in both cardiac MR imaging and computed tomography (CT) goes back to studies published in the late 1970s. In the initial observations that established this concept, iodinated contrast media and CT of extirpated canine hearts with acute and chronic myocardial infarctions were used. Ex vivo CT of hearts with acute infarction demonstrated attenuation of the infarcted tissue that was dramatically higher than that of normal myocardium and that conformed to the site of increased uptake of technetium pyrophosphate (an infarct-avid radionucleotide) and the regional deficit of the distribution of thallium 201 ( $^{201}\text{Tl}$ , a metabolic marker) (1,2) (Fig 1). The region of enhancement closely corresponded to the spatial extent of myocardial infarction as demarcated at histochemical morphometry (triphenyl tetrazolium chloride staining) (Fig 1). Iodine and technetium 99m ( $^{99\text{m}}\text{Tc}$ ) pyrophosphate had the greatest concentration at the center of the infarct; a lower concentration at the periphery suggested a border zone of ischemic injury (Fig 2) (1). The enhancement of acute infarctions was later shown in the in situ beating heart by using a prototype electrocardiography (retrospective)-gated CT scanner in the early 1980s (3–5).

The concept of preferential and persistent enhancement of myocardial infarctions by gadolinium chelates was established by using MR imaging of canine hearts extirpated 5 minutes after administration of gadolinium-based contrast media (6,7). Shortly thereafter, the phenomenon of delayed contrast enhancement of acute myocardial infarctions was demonstrated in the in situ canine heart on electrocardiography-gated T1-weighted MR images (Fig 3) (8). By using electrocardiography-gated MR imaging of the intact animals, it was also shown that differential distribution of gadolinium-based contrast media could also be used to distinguish between reperfused and nonreperfused myocardial

infarction (8); this method could help identify a no-reflow zone (microvascular obstruction). Early animal studies in which varying durations of ischemia were induced showed no delayed enhancement of reversibly injured myocardium (ischemia duration, <15 min) but delayed enhancement only of irreversibly injured myocardium (6–21).

The initial reports identifying differential gadolinium enhancement of myocardial infarctions in patients were published in the late 1980s (22,23).

de Roos and co-workers (22) recognized different enhancement patterns in patients with occlusive infarction and those with reperfused infarction. Improvements in cardiac MR technology, along with the development of a sequence to greatly improve contrast between normal myocardium and infarction, stimulated widespread clinical application of gadolinium-enhanced MR imaging for demonstrating the presence, transmural extent, and size of myocardial infarctions. The MR sequence inversion-recovery gradient-echo imaging to null normal myocardial signal provided enormous contrast between the infarct and adjacent normal myocardium, which enabled ease and reliability of image interpretation (24).

### Present

#### Experimental Basis and Physiologic Mechanism of Delayed Gadolinium Enhancement of Myocardial Infarction

*Physiologic mechanism of delayed and persistent enhancement of damaged myocardium.*— Currently used iodinated and gadolinium contrast media have a similar molecular size, which causes them to distribute rapidly in the extracellular space of the myocardium. These

#### Published online

10.1148/radiol.11091882 Content codes: **CA** **MR**

Radiology 2011; 261:358–374

#### Abbreviations:

LV = left ventricle  
RV = right ventricle

Potential conflicts of interest are listed at the end of this article.

contrast media are excluded from normal myocardial cells. The differences in distribution volume for ischemically injured and normal myocardium were determined by Wendland et al (25) and Pereira et al (18,19). After administration of a gadolinium chelate, ratios of the difference in longitudinal relaxation rates for myocardium and blood at a time of equilibration of contrast medium distribution can be calculated by using repetitive echo-planar imaging in experimental animals (25). From these ratios, the fractional distribution volume of contrast material was estimated for normal and injured myocardium (Fig 4). The fractional distribution volume was about 0.2 in normal myocardium and greater than 0.9 in infarcted myocardium (25–27). These observations indicate that gadopentetate dimeglumine distributes in the extracellular space of normal myocardium but is excluded from the myocardial cell. On the other hand, the contrast medium distributes in the extra- and intracellular spaces after loss of myocardial membrane integrity in the infarcted region (Fig 5). In a series of experiments in rats with coronary occlusion of varying duration (20–60 minutes) followed by reperfusion, the  $\Delta R1$  ratios and fractional distribution volumes progressively increased with increasing severity of myocardial injury (26) (Fig 4). Moreover, the distribution volume of gadolinium-based contrast medium was lower at the periphery than at the core of the infarction, demonstrating the peripheral or periinfarction or marginal zone of injury. In animals with occlusion of 20 minutes duration, the distribution volume increased to 32%, which was greater than the extracellular space of normal myocardium (19%). In these animals with no histochemical evidence of infarction, the modestly greater distribution volume presumably represented myocardial edema. The fractional distribution volume in the peripheral zone of animals with occlusion of 30–60 minutes duration, which caused myocardial infarction, was similar to the edematous myocardium of animals without histochemical evidence of infarction. These findings suggest that delayed gadolinium-enhanced

MR can define a peripheral or periinfarction zone of edema, as well as necrotic myocardium.

The mechanism of enhancement of myocardial scar in chronic infarction and other myocardial diseases is also likely due to expansion of the extracellular space compared with normal myocardium. Fibrosis (scar) has a larger extracellular space than does normal myocardium, which helps explain the regional enhancement of chronic healed infarctions. This is also likely the explanation for delayed enhancement in hypertrophic and other cardiomyopathies. Infiltrative myocardial diseases such as cardiac amyloidosis increase the extracellular space due to the infiltration. Some other myocardial pathologic conditions such as myocarditis may increase the distribution volume by means of a combination of edema and myocardial cell death.

*Ischemic zone and peripheral zone.*— By using multiple MR sequences with and without gadolinium enhancement, several zones can be defined in a region of ischemic myocardial injury: the ischemic zone, the infarction core of necrosis, the peripheral infarction zone, and the microvascular obstruction zone (Fig 6). The ischemic zone is defined as the ischemic area at risk for infarction after a coronary artery occlusion. T2-weighted black blood imaging with fat saturation can be used to detect the area at risk, which shows high signal intensity with this imaging sequence; this reflects myocyte edema as a result of the ischemic injury (28). Areas of myocardial infarct also show high signal intensity on these T2-weighted images but can be differentiated from the area at risk on the basis of the high signal intensity on delayed-enhancement images.

The delayed-enhancement areas consistent with nonviable myocardium are not homogeneous. Instead, delayed-enhancement areas may show a heterogeneous peripheral rim, called the *peripheral zone*, with lower signal intensity than that of the infarct core. The peripheral zone has been defined in several ways both in animal experiments (27) and in clinical studies (29,30). In animals, the peripheral zone was desig-

nated as signal intensity 2–4 standard deviations above that of normal remote myocardium at 5 minutes after gadolinium chelate injection at T1-weighted imaging. In clinical studies with patients, the peripheral zone was described in two ways: Yan and co-workers (29) defined a central, highly intense, myocardial infarct core as an area with signal intensity greater than 3 standard deviations above the intensity of the remote noninfarcted myocardium, whereas 2–3 standard deviations above normal was designated as the peripheral zone. Azevedo et al (30) defined the infarct core as an area with signal intensity above 50% of the maximal signal intensity measured in the delayed-enhancement myocardium. Any areas of signal intensity higher than the peak signal intensity of the remote myocardium but lower than 50% of the peak intensity as measured in the core zone was designated as peripheral zone.

As previously described in animal studies, the peripheral zone represents a region of nonviable myocardial cells interspersed with viable myocytes (15). The areas of lesser delayed enhancement corresponding to a peripheral zone are not only seen in the periphery of the infarct zone, but can also be detected in more central locations with areas of dense myocardial infarction (31–33).

*Infarction size.*— The zone of enhancement after gadolinium chelate administration has been found to have a close relationship to the size of the myocardial infarction demarcated at post-mortem histochemical staining (histochemical morphometry) in animals (14,15, 25–27,34). On T1-weighted images acquired several hours after coronary artery occlusion and reperfusion, the enhanced region demarcated by gadolinium enhancement was larger than, but proportional to, the infarction volume determined at histochemical morphometry. The difference in infarction volume as defined on gadolinium-enhanced images and true infarction size was considered to be due to a peripheral zone of potentially salvageable myocardium. In support of this notion, gadolinium-enhanced spin-echo MR imaging demonstrates a moderate peripheral zone on images acquired

Figure 1

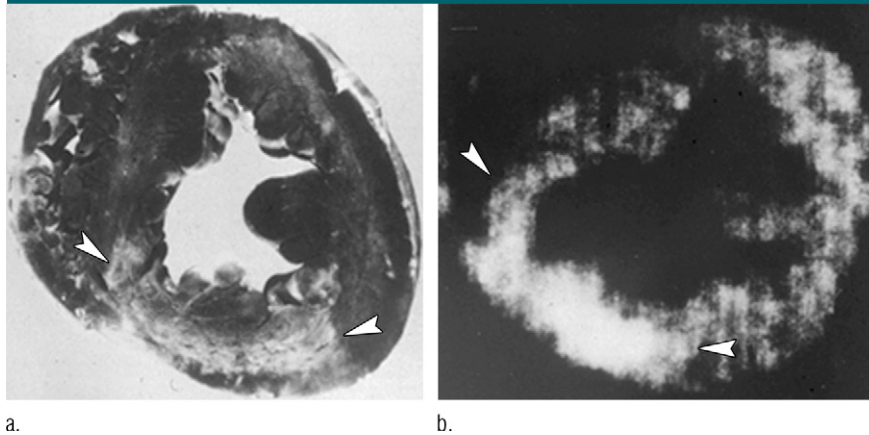


**Figure 1:** (a) Transverse myocardial slice shows region of acute myocardial infarction (arrowheads). (Triphenyl tetrazolium chloride stain.) (b) CT scan of canine heart at same level as a shows delayed enhancement by iodinated contrast medium injected about 10 minutes before extirpation of the heart. (Reprinted, with permission, from reference 2.)

on the day of coronary occlusion, but this zone diminishes in size or disappears on images acquired 2–6 weeks after infarction. Presumably, the peripheral zone consists of edematous (reversibly injured) but not necrotic myocardium. In further support of this conclusion is the observation that MR images obtained 24 hours after reperfusion of acute myocardial infarction show a different size of the enhanced zone when gadopentetate dimeglumine is used than when the necrosis-specific contrast medium gadophrin-2 is used (14,15). The size of the gadophrin-2-enhanced regions exactly matched the size of infarction defined at histochemical morphometry, while the area defined by gadopentetate dimeglumine was substantially larger. Other studies have also shown that the size of the gadophrin-2-enhanced region exactly matched the infarction size from histochemical morphometry (20,34,35).

Using an inversion-recovery gradient-echo MR imaging (viability) sequence, Judd et al (12) found little difference between the enhanced region and infarction size at postmortem examination. Kim et al (13) reported an exact match between the enhanced zone on viability sequence images and infarction size at histochemical morphometry in dogs. In support of this notion that enhancement of any degree occurs only in

necrotic myocardium, Kim et al (13) showed a “match” between 2-mm-thick tissue slices stained with triphenyl tetrazolium chloride and postmortem MR images in hearts extirpated at the optimal delay after gadopentetate dimeglumine administration. On the basis of the results of these experiments, they concluded that in the setting of acute infarction with or without reperfusion, the spatial extent of infarction on inversion-recovery gradient-echo images is identical to the extent of myocardial necrosis. They attributed differences in size between the enhanced region and postmortem histochemical morphometry of infarction volume as previously reported to be due to partial volume errors.

Recognizing that partial volume error could potentially contribute to apparent differences between enhanced volume on in vivo MR images and true infarction volume at postmortem examination, Arheden et al (27) assessed tissue distribution of a radioactive co-gener of gadolinium dimeglumine,  $^{99m}\text{Tc}$ -labeled pentetic acid, in the presence of acute myocardial infarction. On autoradiographs of 10- $\mu\text{m}$ -thick myocardial slices, three zones of radionuclide distribution were evident: a normal myocardial zone, a zone at the center with radioactivity 4 standard deviations higher

than that of normal tissue, and a zone at the periphery of the infarct with radioactivity 2 standard deviations higher (Fig 7). These investigators concluded that a peripheral zone of delayed enhancement exists that cannot be attributed to partial volume effects on MR images of 3–5-mm thickness. It remains conjectural whether the inversion-recovery gradient-echo technique, which attempts to maximize contrast between infarcted and normal myocardium by nulling the signal of normal myocardium, can render the peripheral zone invisible.

**Acute versus chronic infarctions.**— Both acute (necrosis) and chronic (scar) myocardial infarctions show delayed enhancement after administration of gadopentetate dimeglumine and other contrast media that are distributed in the extracellular space (13). Therefore, when gadopentetate dimeglumine or other extracellular contrast media are used, acute and chronic infarctions cannot be distinguished on the basis of the presence of enhancement alone. Morphologic features such as wall thinning can be used to presume that an area of enhancement represents scar rather than acute necrosis.

Acute and chronic infarctions can also be differentiated by combining T2-weighted imaging with delayed gadolinium-enhanced imaging (36). T2-weighted images show a high-signal-intensity region larger than that on delayed gadolinium-enhanced images in cases of acute infarction; the difference between the two zones is presumed to be a peripheral region of reversible injury where there is myocardial edema but not infarction. Chronic infarction (scar) does not display hyperintensity on T2-weighted MR images.

Differentiation between acute and chronic myocardial infarction can also be accomplished by using both extracellular gadopentetate dimeglumine, which has low molecular weight, and another gadolinium-based contrast medium with larger molecular size (pseudo-blood pool medium). Low-molecular-weight gadolinium-based contrast media cause delayed enhancement of acute and chronic myocardial infarctions. Larger molecular weight contrast media cause enhancement

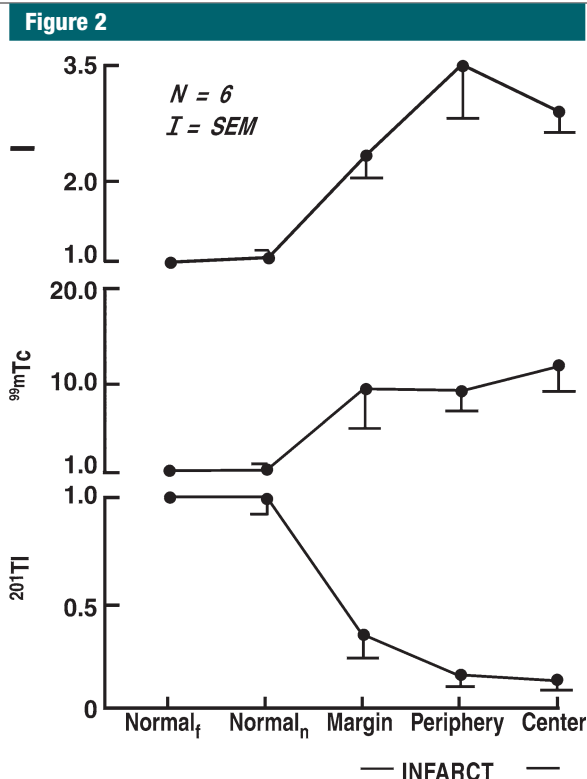


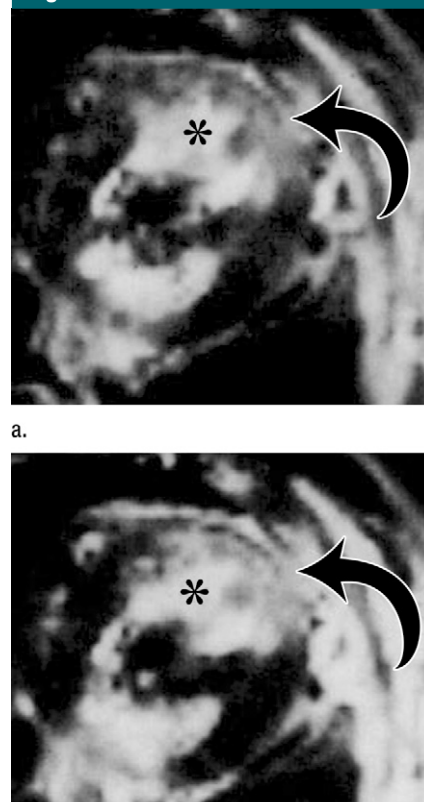
**Figure 2:** Relative concentration or radioactivity of iodine,  $^{99m}\text{Tc}$  pyrophosphate, and  $^{201}\text{Tl}$  in various sites of transverse myocardial tissue slices. Values are expressed as proportion of concentration in normal myocardium, considered to have relative concentration of 1.0. *Normal<sub>f</sub>* = normal myocardium far from infarction; *Normal<sub>n</sub>* = normal myocardium near infarction. Samples were obtained from the margin, periphery, and center of infarction. Iodinated contrast medium had a spatial distribution approximating that of infarction-avid  $^{99m}\text{Tc}$  pyrophosphate and diametric to myocardial perfusion tracer  $^{201}\text{Tl}$ . *SEM* = standard error of the mean. (Reprinted, with permission, from reference 1.)

of acute but not chronic myocardial infarction (37). In acute infarction, small intramyocardial blood vessels are destroyed so that blood pool contrast media escape the vascular space in the infarct but not in normal myocardium; hence, blood pool media have a larger distribution volume in the acute infarction. Neovascularization in the scar retains the intravascular distribution of the high-molecular-weight contrast medium.

**Variation in infarct size over time.**—Infarction size in experimental animals, as demarcated by enhancement of the ischemically damaged region on in vivo MR images, is largest in the first 2 days after coronary artery occlusion and de-

creases in size over the ensuing weeks to months according to a number of reports (38–40). Most of the studies in animals show a decrease in infarction size on gadolinium-enhanced T1-weighted spin-echo MR images acquired from the 1st days to several weeks after occlusion-reperfusion. On the other hand, other investigators (13), using sequential imaging in dogs, have found little or no decrease in infarction size from day 1 after ischemic injury to several weeks later. These studies have used the inversion-recovery gradient-echo sequence with nulling of signal of normal myocardium at 10–15 min after injection of gadolinium chelate. It is proposed that these discrepant observa-

**Figure 3**



**b.**

**Figure 3:** Electrocardiography-gated spin-echo MR images (repetition time msec/echo time msec, 600–900/60), acquired (a) before and (b) 5–10 minutes after intravenous injection of gadolinium chelate in a dog with acute myocardial infarction. Infarction in the anteroapical region (arrows) shows enhancement relative to that of normal myocardium. Intracavitary high signal intensity (\*) is due to stasis of blood adjacent to akinetic segment of left ventricle (LV). (Adapted and reprinted, with permission, from reference 8.)

tions may be related to the imaging sequence because, by maximizing contrast between normal and infarcted myocardium, images obtained with the inversion-recovery gradient-echo sequence may not depict the peripheral edematous zone.

### Clinical Application in Ischemic Heart Disease

Delayed enhancement indicative of myocardial infarction is always subendocardial and extends to a variable degree through the wall, corresponding to the

Figure 4

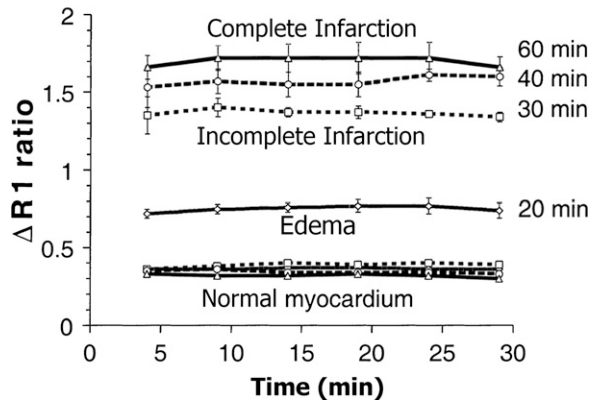


Figure 4: Graph shows differences in longitudinal relaxation time ( $\Delta R1$ ) ratio of myocardium to blood for myocardial ischemic injuries of increasing severity. The ratio is an estimate of distribution volume of the contrast medium (gadodiamide). The x-axis represents time after injection. (Adapted and reprinted, with permission, from reference 26.)

Figure 5

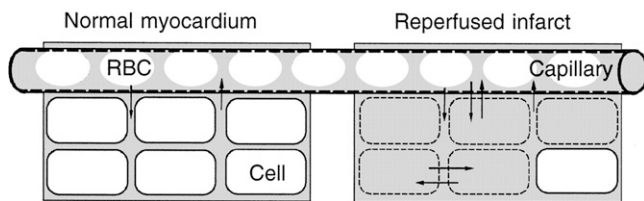


Figure 5: Diagram shows extracellular distribution of contrast medium in normal myocardium and reperfused infarcted myocardium. In normal tissue, gadopentetate dimeglumine and other contrast media (gray areas) distribute in the extracellular space and are excluded from the intracellular space. After infarction, cellular membrane integrity is disrupted, so media enters intracellular space, markedly increasing the distribution volume. RBC = red blood cell. (Reprinted, with permission, from reference 27.)

distribution area of a major coronary artery (Figs 8, 9). Multiple studies (41–53) in patients have shown that delayed-enhancement MR images can demonstrate the presence, location, and transmural extent of acute and chronic myocardial infarctions. An international multicenter study (54) reported a sensitivity of 99% for detection of acute infarction and 94% for detection of chronic infarction. Small infarctions, even those without Q waves, have been readily detected on delayed-enhancement MR images (55–57). Delayed-enhancement MR imaging depicts small infarcts that can be missed at  $^{99m}\text{Tc}$  sestamibi single photon emission computed tomography

(SPECT) performed 7 days after percutaneous transluminal coronary angioplasty in patients with acute coronary syndrome (48). Delayed-enhancement MR imaging is more accurate than SPECT for detection of subendocardial infarction (48,56).

In patients with acute myocardial infarction, the infarction size, as defined by the extent of delayed gadolinium enhancement, correlated with clinical measures of infarction severity such as peak troponin level and left ventricular (LV) ejection fraction at late follow-up (49). In those patients reevaluated an average of 5 months after the acute event, the size of the area of delayed enhance-

Figure 6

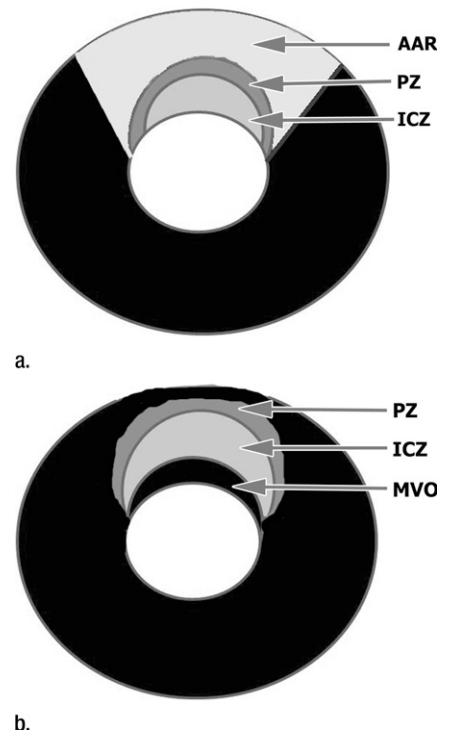
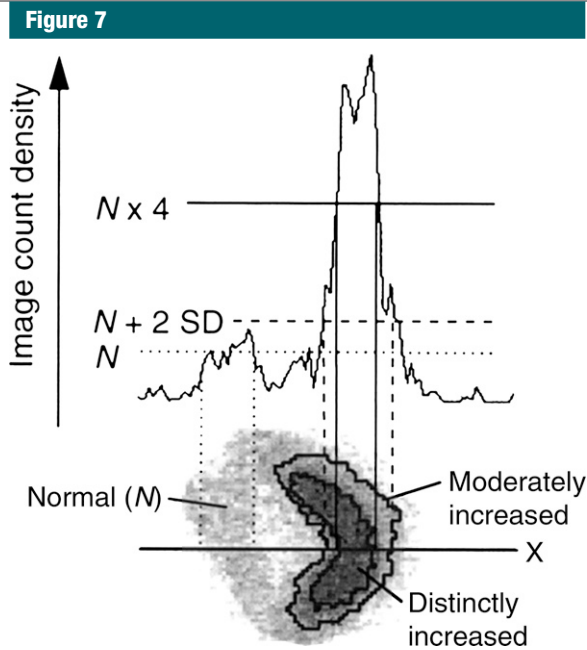


Figure 6: Diagrams show delayed-enhancement zones. ICZ = infarct core zone, PZ = peripheral zone. (a) Subendocardial myocardial infarction. AAR = area at risk. (b) Transmural myocardial infarction with microvascular obstruction (MVO).

ment (infarction size) decreased almost 40% (49).

Schulz-Menger et al (58) sequentially evaluated delayed-enhancement MR images obtained from 1 hour to 180 days after induction of acute myocardial infarction by means of septal artery embolization for the treatment of hypertrophic cardiomyopathy. Delayed enhancement was observed 1 hour after embolization and persisted through the entire follow-up. The area of enhancement was significantly larger at days 7–14 than it was later. Other studies (45,49) have also indicated a substantial decrease in infarction mass from the acute to the chronic state.

*Delayed-enhancement MR for predicting recovery of LV function.*— A number of studies (41,44–46,48–50,59) have shown that delayed-enhancement MR imaging findings can be predictive of the potential for recovery of function



**Figure 7:** Autoradiographic distribution of  $^{99m}\text{Tc}$  pentetic acid on 10- $\mu\text{m}$  slices from canine reperfused myocardial infarction. There are three distinct zones of radioactivity: normal ( $N$ ); center of infarction (4 standard deviations [ $SD$ ] higher than normal); and border, or marginal, zone of infarction (2 standard deviations higher than normal). (Reprinted, with permission, from reference 27.)

in LV dysfunctional segments in chronic ischemic heart disease. Ramani et al (47) reported more than a decade ago that the presence or absence of delayed enhancement correlated closely with nonviability or viability in LV segments which were akinetic or dyskinetic at rest in patients with chronic ischemic heart disease.

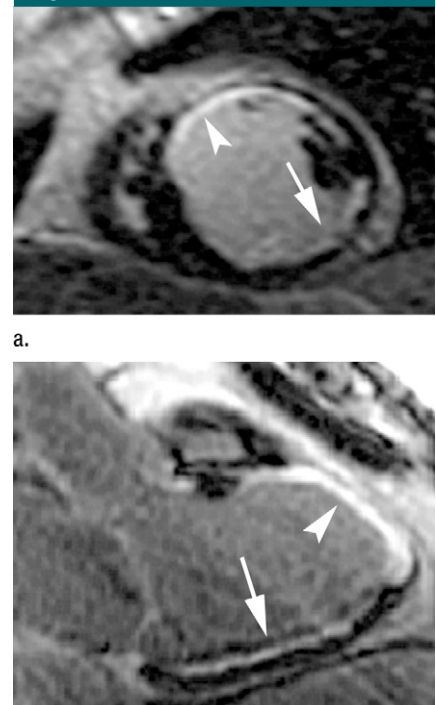
Recovery of contraction in regions with dysfunction after revascularization has been related to the transmural extent of enhancement in patients with acute infarction, chronic ischemic dysfunction, and ischemic cardiomyopathy. Choi et al (41) found, in 24 patients with first infarction and successful early revascularization, that the transmural extent of enhancement 7 days after the acute event was predictive of recovery of wall thickening and ejection fraction at 8–12 weeks. The best predictor of global contraction as reflected in ejection fraction and mean wall thickening score was the extent of dysfunctional myocardium that had no delayed en-

hancement or delayed enhancement of less than 25% of wall thickness. Another group (53) found that late improvement in regional function was more closely predicted by a thickness of normal myocardium of greater than 5.5 mm in dysfunctional segments with delayed enhancement.

Kim et al (44) used transmural extent of delayed enhancement to predict recovery of regional function in dysfunctional segments in patients evaluated before and several months after surgical revascularization. A cutoff of 50% transmural delayed enhancement was a practical gauge of reasonable likelihood of recovery of regional function after revascularization—less than 50% transmural predicted recovery in 53% of segments, while greater than 50% transmural was associated with recovery in only 8% of segments. Less than 25% transmural predicted residual viability in 82% of segments.

*Predictions of viability compared with other tests.*—Delayed-enhancement

**Figure 8**

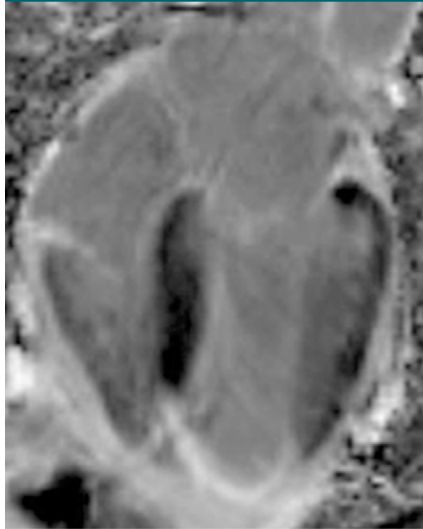


b.

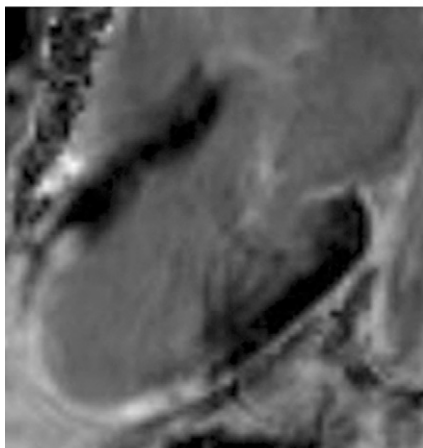
**Figure 8:** Delayed-enhancement inversion-recovery gradient-echo MR images (5/2.3) in (a) short-axis and (b) vertical long-axis planes in patient with subendocardial infarction in diaphragmatic segment (arrow) and transmural infarction in anteroseptal segment (arrowhead) of LV. (Image courtesy of Steven Wolff, MD, PhD, New York, NY.)

MR imaging and positron emission tomography (PET) for determination of myocardial viability after prior infarction have also been compared (60,61). The sensitivity and specificity of delayed-enhancement MR images for identification of LV segments flow metabolism defects on matched PET scans were 0.96 and 0.86, respectively. Infarct on delayed-enhancement MR images and infarct mass on PET scans correlated well: 11% of segments defined as viable on PET scans showed infarct on delayed-enhancement MR images, suggesting that the latter are more sensitive for detection of infarction because of the better spatial resolution of MR images. Fluorodeoxyglucose (FDG) uptake of more than 50% at PET and delayed gadolinium enhancement at MR with a peripheral nonenhancing rim thicker than 4.5 mm

Figure 9



a.



b.

**Figure 9:** Delayed-enhancement inversion-recovery gradient-echo MR images (5/2.3) in (a) horizontal and (b) vertical long-axis planes show transmural delayed enhancement in anteroapical and posteroapical segments of the LV.

correlated well for prediction of viability at approximately a year after revascularization (61). FDG uptake greater than 50% and 4.5-mm-thick rim outside the region of delayed enhancement enabled identification of 85% of LV segments that recovered function.

Demonstration of residual contractile function in dysfunctional segments in response to dobutamine stimulation at cine MR imaging has been shown to be better than delayed-enhancement

MR imaging alone for prediction of recovery of segmental function 3 months after revascularization (59). The advantage of dobutamine-stimulation cine MR was shown in segments with transmural delayed enhancement of 1%–75%. In patients with previous myocardial infarction in more than 50% of dysfunctional segments with transmural delayed enhancement of 25%–75% showed contractile reserve on dobutamine-stimulation echocardiography (62).

*Delayed enhancement in the absence of history of myocardial infarction.*—Delayed-enhancement MR imaging in 195 patients suspected of having coronary artery disease but with no history of myocardial infarction demonstrated delayed enhancement in nearly 23% of patients (63). During a 16-month follow-up period, delayed enhancement was the strongest predictor of mortality and major adverse cardiac events, as compared with clinical data, coronary sclerosis at angiography, or LV end-systolic volume index and ejection fraction. Even a small area of delayed enhancement (<2% of LV mass) was associated with a greater than seven-fold increase in risk for a major adverse cardiac event. Thus, delayed-enhancement MR imaging was proposed as a test to improve risk assessment in patients with possible coronary artery disease. It is conceivable that small “silent” infarct may be a precursor of a large infarct leading to major morbidity and mortality.

Delayed-enhancement MR imaging in 248 randomly recruited 70-year-old subjects demonstrated focal delayed enhancement in 24% of the subjects (64). In 49 of 60 patients, the site was subendocardial, indicating prior undetected myocardial infarction. The LV ejection fraction was lower and the mass was greater in those with unrecognized myocardial infarction than in the rest of the elderly subjects.

*Prognostic implications of delayed enhancement with microvascular obstruction.*—Most acute myocardial infarctions are associated with delayed enhancement in a subendocardial or transmural distribution. Acute infarction with microvascular obstruction (destruc-

tion) is recognized as midwall and/or epicardial enhancement surrounding a subendocardial region of low signal intensity (Figs 6, 10). This pattern is associated with greater infarct mass, lower ejection fraction, more adverse cardiac events early and late, and more severe late LV remodeling (43,65–69). Microvascular obstruction has a close direct relationship to infarction size and extent of transmural (69).

*Clinical implications of the peripheral zone.*—Infarction size, as defined on the basis of voxels with signal intensity greater than 2 standard deviations above that of normal myocardium on delayed-enhancement MR images, was shown to be stronger predictor of inducible ventricular arrhythmia than is LV ejection fraction (70). In this initial report, central and peripheral zones of infarction were not discriminated.

More recently, sequential studies were performed in 144 patients after myocardial infarction to evaluate the prognostic role of peripheral zone findings (29). The peripheral zone was calculated by using the method described above. Patients with a larger peripheral zone had increased risk for mortality from all causes and cardiovascular mortality after a follow-up of 2.4 years. This association was independent of LV ejection fraction and LV volume. There was no correlation between the total size of the infarct or transmural and the risk of death. The extent of the peripheral zone and the LV end-systolic volume index were the strongest predictors of mortality. The authors postulated that the association between extent of the peripheral zone and mortality is likely due to an increased substrate of viable myocyte “islands” in the peripheral zone, which could increase the risk for cardiac arrhythmia.

In agreement with the above notion, Schmidt and co-workers (71) have shown that extensive tissue heterogeneity correlates with increased ventricular irritability, as demonstrated with programmed electric stimulation. The presence of inducible ventricular arrhythmia is a marker for increased risk of lethal arrhythmia in patients with chronic myocardial infarction.

Figure 10

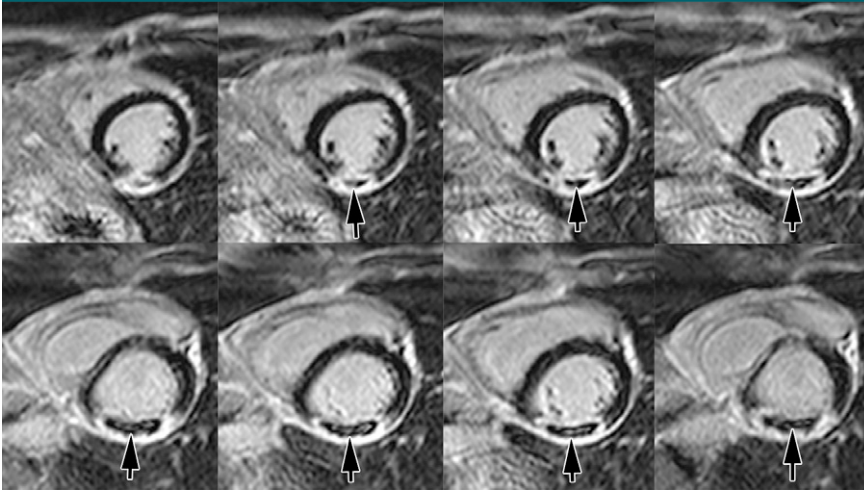


**Figure 10:** Delayed-enhancement inversion-recovery gradient-echo short-axis MR images (5/2.3) acquired from near the apex (top left) to near the base (bottom right) of the LV show delayed enhancement of the periphery and lack of enhancement in the subendocardial layer (arrows) of the posterior segment of the LV. The low-signal-intensity subendocardial region with infarction is predictive of microvascular obstruction. (Image courtesy of Hajime Sakuma, MD, Mie, Japan.)

### Clinical Application in Nonischemic Acquired Heart Disease

**Myocarditis.**— The mechanism of delayed enhancement in the early phase of myocarditis is myocardial necrosis, while in the late phase it is likely due to fibrosis (72). The distribution of delayed enhancement in patients with myocarditis typically spares the endocardial region and affects the subepicardial or midwall areas (Fig 11) (Table). The distribution can be diffuse or multifocal, or it can be regional. Marnholdt et al (73) have suggested that certain LV sites may be characteristic for viral agents. Parvovirus most frequently caused delayed enhancement of the subepicardial layer of the lateral wall, and human herpes virus caused enhancement in the ventricular septum.

Multiple studies have shown high specificity of delayed enhancement for the diagnosis of myocarditis (72–76) with differences in respect to acute and chronic disease. However, sensitivity has been variable in the literature (72–74,77–79). A possible explanation is that myocarditis can be associated with small scattered areas of necrosis that are below the resolution of delayed-enhancement MR images, as opposed to

regional contiguous myocardial necrosis such as that which occurs in ischemic injury. Delayed enhancement can be detected in 70% of patients with chronic myocarditis, predominantly enhancement that involves the midwall (67.5%) but also that which affects the subepicardium (37.5%).

The prognostic value of delayed enhancement in the setting of myocarditis is not clear. A correlation between gadolinium enhancement ratio and cardiac dysfunction after a 3-year follow-up was demonstrated in one study (80).

**Dilated cardiomyopathy.**— Delayed-enhancement MR images can be useful for distinguishing between ischemic cardiomyopathy and idiopathic dilated cardiomyopathy. McCrohon et al (81) showed that 59% of patients with dilated cardiomyopathy and normal coronary arteries at conventional angiography showed no delayed enhancement, whereas 28% of patients had a midwall distribution of delayed enhancement that is consistent with a nonischemic cause. A minority of patients in that study had delayed enhancement with an ischemic distribution, which was thought to be related to a recanalized coronary obstruction. Recently, the extent of fibrosis depicted on

Figure 11

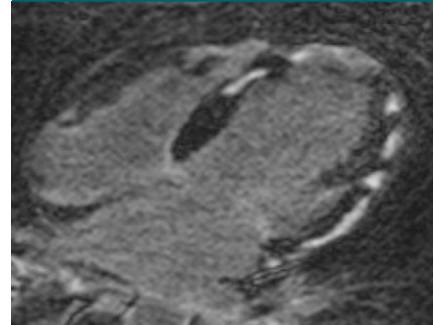


**Figure 11:** Delayed-enhancement inversion-recovery gradient-echo MR image (repetition time msec/echo time msec/inversion time msec, 5/2.3/280) in horizontal long-axis plane acquired 15 minutes after injection of a gadolinium chelate in a patient with viral myocarditis. Note enhancement in midwall of septum, subepicardial layer of lateral LV wall, and apex of the right ventricle (RV).

delayed-enhancement MR images has been associated with increased risk of intraventricular systolic dyssynchrony in patients with nonischemic dilated cardiomyopathy (82).

**Hypertrophic cardiomyopathy.**— Delayed enhancement has been reported in 81% of patients with hypertrophic cardiomyopathy. The distribution is typically in the ventricular septum adjacent to the connection with the RV free wall (83). Areas of delayed enhancement had a midwall or subepicardial distribution but never involved the subendocardial region. Delayed enhancement also occurs in the region of most severe hypertrophy, such as the asymmetrically hypertrophied ventricular septum (Fig 12).

Delayed enhancement in patients with hypertrophic cardiomyopathy is most likely related to ischemic injury with myocardial collagen replacement (84,85). An alternative theory states that areas of myocardial disarray characteristically seen in hypertrophic cardiomyopathy at the junction of the ventricular septum and the RV free wall could also result in increased extracellular space and accumulation of contrast medium shown on delayed enhancement MR images (86). Ex vivo studies have demonstrated an association between fibrosis and sudden death in patients with hypertrophic cardiomyopathy

### Patterns of Delayed Enhancement in Nonischemic Heart Disease

Disease	Transmural Distribution	Commonly Involved Region
Myocarditis	Subepicardial or midwall	Variable
Dilated cardiomyopathy	Midwall	None
Hypertrophic cardiomyopathy	Midwall or subepicardial	Areas of most severe hypertrophy; ventricular-septal connection points
Sarcoidosis	Subepicardial or midwall	Right ventricular side of the septum; basal anterolateral and anteroseptal
Amyloidosis	Subendocardial, midwall, or subepicardial	Global (when subendocardial)
Arrhythmogenic right ventricular dysplasia	Transmural, subepicardial, or subendocardial	Right ventricular free wall; right ventricular side of the septum
Anderson-Fabry	Midwall	Basal inferolateral
Chagas	Transmural or subepicardial	Apical; basal inferolateral
Churg-Strauss	Subendocardial, possibly midwall or subepicardial	Ventricular septum
Lyme	Midwall	Basal anteroseptal
Endomyocardial fibrosis	Subendocardial	None

(87–89). Clinical studies have also demonstrated an association between the presence of myocardial fibrosis and the risk of developing ventricular arrhythmias. Adabag et al (90) showed that patients with hypertrophic cardiomyopathy and any degree of delayed enhancement have a seven-fold higher risk of nonsustained ventricular tachycardia (when they are being observed with 24-hour Holter monitoring) compared with patients without evidence of delayed enhancement. Surprisingly, the transmural extent of the delayed enhancement and the percentage of LV myocardium with delayed enhancement were not associated with ventricular arrhythmias. Satoh and co-workers (91) have demonstrated that the presence of delayed enhancement is not only correlated with prevalence of ventricular tachycardia on Holter monitoring, but is also associated with higher New York Heart Association functional class, impaired global LV function, conductance disturbance, abnormal Q waves, and giant T waves.

The authors of another report demonstrated that patients with hypertrophic cardiomyopathy and progressive LV dilatation, consistent with progressive disease, have more extensive delayed enhancement than do patients with stable disease (92). The same study also showed greater extent of enhancement in patients with two or more risk factors for sudden death.

**Sarcoidosis.**—Cardiac involvement has a reported prevalence of 7% in pa-

tients with pulmonary sarcoidosis (93). However, 20%–30% of postmortem examinations revealed cardiac involvement in sarcoidosis (94,95).

Delayed-enhancement MR images in patients with myocardial sarcoidosis have shown diffuse or focal enhancement in the middle of the myocardial wall or in the subepicardial region (Fig 13) (96,97). Delayed enhancement of the RV side of the septum is considered to be a characteristic feature (98). It has been reported that delayed enhancement in sarcoidosis involves predominantly basal segments of the LV, with the anteroseptal and anterolateral segments most frequently affected (99).

Matoh et al (100) identified delayed enhancement in only five (42%) of 12 patients with cardiac sarcoidosis, whereas Ichinose et al (97) reported this finding in 10 (91%) of 11 patients with cardiac sarcoidosis. Smedema and colleagues (101) demonstrated a correlation between extent of delayed enhancement and disease duration, ventricular dimensions and function, severity of mitral regurgitation, and presence of ventricular arrhythmias. Ichinose et al (97) also showed a significant correlation between global extent of myocardial enhancement with increased LV volume and decreased LV contractility.

**Amyloidosis.**—For the diagnosis of amyloidosis, delayed-enhancement MR imaging has a specificity of 94% and a sensitivity of 80%, with endomyocardial biopsy as the standard of reference (102). Global subendocardial delayed

enhancement, the so called amyloid late gadolinium-enhancement pattern, has been described in up to 80% of patients with amyloidosis (102–104) (Fig 14). Other distributions of delayed enhancement have been reported as patchy midwall, subendocardial, or subepicardial distribution. Most patients with global subendocardial delayed enhancement also showed papillary muscle involvement.

For acquisition of delayed-enhancement MR images, establishment of the optimal inversion time to null the signal of normal myocardium in patients with amyloidosis can be problematic (103). As proposed by Maceira and colleagues (103), multiple inversion times need to be used to determine the nulling point of normal myocardium, since areas with amyloid deposition typically demonstrate an inversion time shorter than that of the blood pool. In addition, contrast between normal myocardium and areas with amyloid deposition fades approximately 8 minutes after the administration of gadolinium chelate owing to altered contrast agent kinetics. Therefore, delayed-enhancement MR images in patients with possible cardiac amyloidosis must be acquired between 5 and 8 minutes after the administration of the contrast medium.

The mechanism for delayed enhancement in patients with amyloidosis is controversial. Theories include expansion of the extracellular space due to accumulation of abnormal interstitial protein or myocardial fibrosis due to perivascular amyloid deposition (105,106). The

Figure 12

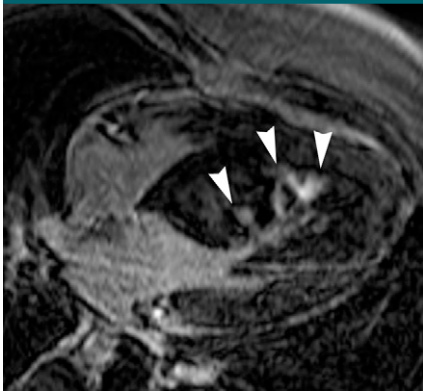


**Figure 12:** Delayed-enhancement inversion-recovery gradient-echo MR image (5/2.3/280) in horizontal long axis plane acquired 15 minutes after injection of a gadolinium chelate in a patient with asymmetric septal form of hypertrophic cardiomyopathy shows enhancement of hypertrophied septum (arrowheads).

former theory is supported by necropsy studies that have demonstrated typical global subendocardial amyloid deposits consistent with the most common distribution pattern seen on delayed-enhancement MR images (107). However, a small study (five patients) in which areas of delayed enhancement and histopathology findings were directly compared showed a significant correlation between the MR imaging abnormality and areas of fibrosis but no correlation with areas of myocardial amyloid deposition (106).

Regarding clinical and prognostic implications of delayed-enhancement MR imaging for amyloidosis, Perugini et al (104) showed that the presence of delayed enhancement has no correlation with clinical, functional, or histologic characteristics of the disease. In agreement, Ruberg et al (108) showed that delayed enhancement is not predictive of survival in a follow-up study of 21 patients with light-chain cardiac amyloidosis. However, that study demonstrated a correlation between delayed enhancement and B-type natriuretic peptide, a marker of heart failure severity.

#### Rare Myocardial Diseases with Delayed Gadolinium Enhancement

**Arrhythmogenic RV dysplasia/cardiomyopathy.**—Delayed enhancement

Figure 13

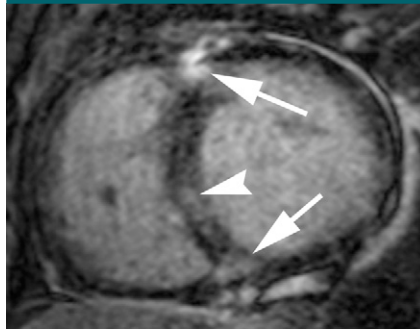


**Figure 13:** Delayed-enhancement inversion-recovery gradient-echo MR image (5/2.3/280) in short-axis plane, acquired 15 minutes after injection of a gadolinium chelate in a patient with myocardial sarcoidosis shows focal transmural delayed enhancement in anterior and posterior margins of the ventricular septum (arrows) and midwall delayed enhancement in center of the ventricular septum (arrowhead).

has been described in areas of fibrofatty myocardial changes in patients with arrhythmogenic RV dysplasia/cardiomyopathy (ARVD/C). Pfluger et al (109) reported delayed enhancement in seven (88%) of eight patients with ARVD/C; then enhancement predominantly involved the RV free wall but also affected the RV side of the ventricular septum. In most patients, it was associated with regional contraction abnormality. In addition, it has been shown that delayed enhancement has an excellent correlation with histopathologic diagnosis of fibrofatty infiltration in patients with ARVD/C (110). Tandri et al (110) showed that the presence of RV delayed enhancement is predictive of inducible ventricular tachycardia at programmed electric stimulation, which suggests a possible role of viability imaging in the prognostic assessment of patients with ARVD/C.

**Anderson-Fabry disease.**—Anderson-Fabry disease is an X-linked disorder of the sphingolipid metabolism, which should be considered in the differential diagnosis of symmetric hypertrophic cardiomyopathy. Delayed enhancement MR imaging demonstrates a typical and consistent pattern and site in patients with Anderson-Fabry disease, which is distinguishable from symmetric hypertrophy caused by hypertrophic cardiomyopathy. The characteristic pattern of

delayed enhancement involves the midwall, sparing the subendocardial region, with a predilection for the inferolateral basal segments of the LV (111).

**Chagas disease.**—Cardiac involvement is very common in chronic Chagas disease, and lymphocytic infiltration of the myocardium is characteristic. Regions of myocardial fibrosis have been shown to enhance strongly on delayed-enhancement MR images, with a transmural, subepicardial, or midwall distribution (112,113). LV inferolateral basal segments and the apical region are the most commonly affected regions. Apical aneurysm of the LV with transmural delayed enhancement is characteristic of chronic Chagas disease. Delayed enhancement is seen more often in patients with advanced disease and worse clinical presentation than in patients with early cardiac involvement. In addition, all patients with ventricular tachycardia due to chronic Chagas disease showed delayed enhancement, suggesting a prognostic role for delayed-enhancement MR imaging in this disease.

**Churg-Strauss syndrome.**—A few case reports have demonstrated delayed enhancement of LV myocardium in Churg-Strauss syndrome. Pattern of delayed enhancement has varied including patchy distribution in subendocardial, midwall and subepicardial regions (114), predominant involvement of the ventricular septum (115) and diffuse subendocardial with papillary muscle involvement (116). Correlation with histopathology showed good match between the regional myocardial enhancement and the eosinophilic infiltrates (114).

**Lyme cardiomyopathy.**—Lyme cardiomyopathy affects between 1.5% and 10% of patients with Lyme disease and typically presents as atrioventricular block (117). Delayed enhancement has been described in a few case reports of patients with Lyme cardiomyopathy. The abnormality on delayed-enhancement MR images involved the midwall region of the basal anteroseptal wall, which is the expected location of the atrioventricular node (118). Decrease in extent of delayed enhancement after 6 weeks of treatment has been shown to be accompanied by improvement of atrioventricular block,

Figure 14

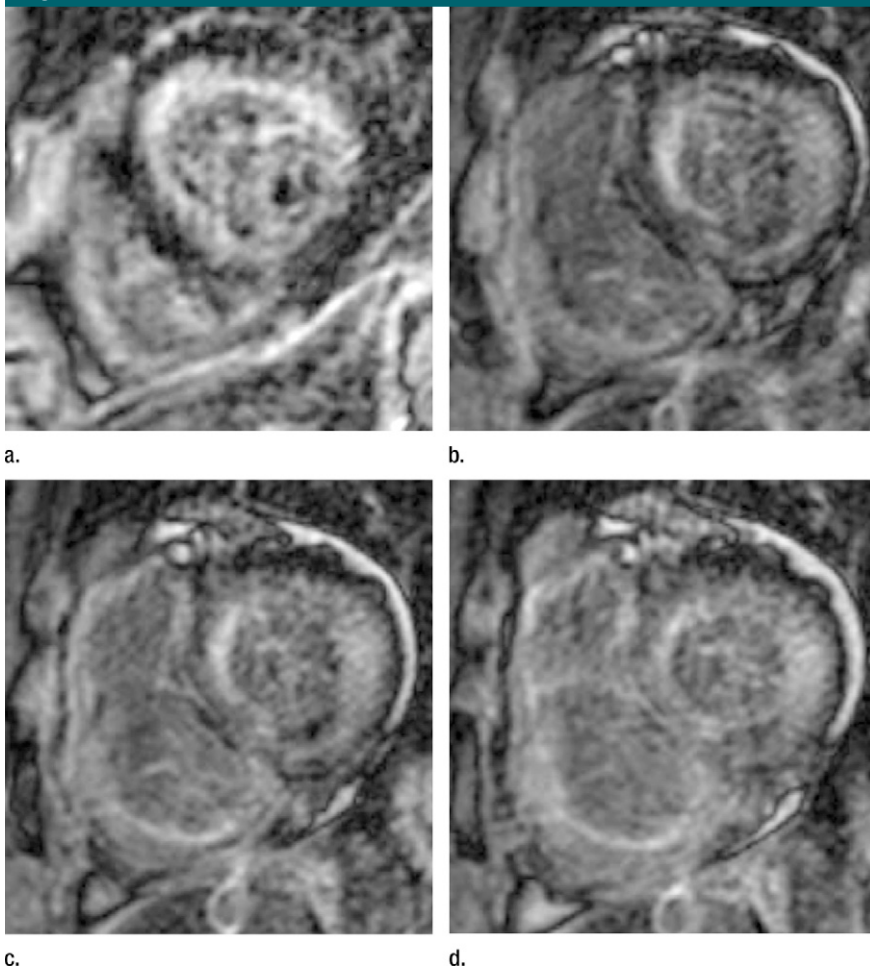


**Figure 14:** (a–d) Delayed-enhancement inversion-recovery gradient-echo MR images (5/2.3/280) in short-axis plane from apex (a) to base (d) acquired 8 minutes after injection of gadolinium chelate in a patient with cardiac amyloidosis show circumferential subendocardial enhancement of both RV and LV myocardium. Note low signal intensity of the blood pool, as typically seen on delayed-enhancement images in patients with amyloidosis.

which suggests a role for delayed-enhancement cardiac MR imaging for follow-up in these patients (118). Complete resolution of the delayed enhancement has been shown after clinical recovery (119).

**Endomyocardial fibrosis.**— Chronic fibrotic stage of endomyocardial fibrosis is characterized by the presence of scar in the subendocardium and chordae tendineae, resulting in congestive heart failure. In a few case reports (120–124), a typical appearance of biventricular delayed enhancement involving the subendocardial region with adjacent non-enhancing mural thrombus has been

demonstrated. Rarely, there may be predominant RV involvement (Fig 15).

#### Postoperative Congenital Heart Disease

After surgical correction of congenital heart diseases, delayed enhancement is frequently seen at sites of prior surgical intervention (Fig 16). However, areas of delayed enhancement have also been demonstrated in myocardium remote from the surgical site.

After correction of tetralogy of Fallot, Oosterhof et al (125) identified delayed enhancement in the RV outflow tract (RVOT) in 17 (71%) of 24 patients. Most patients were adults and

Figure 15

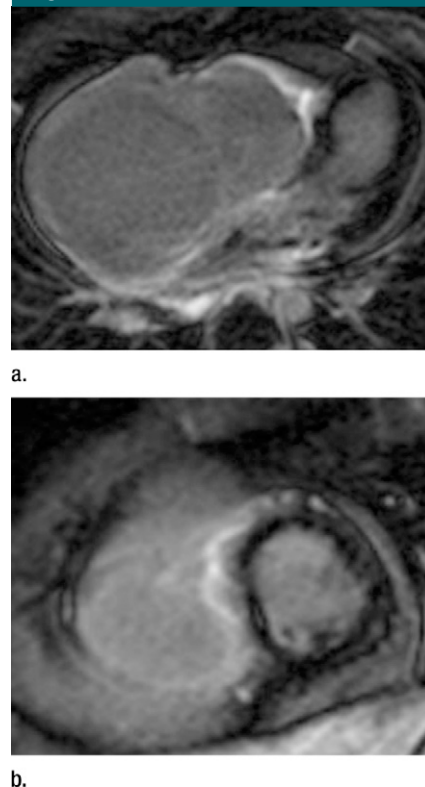


**Figure 15:** Delayed-enhancement inversion-recovery gradient-echo MR images (5/2.3/280) in (a) horizontal long-axis and (b) short-axis planes show delayed enhancement in subendocardial layer of RV in a patient with biopsy-proved endomyocardial fibrosis. There is severe enlargement of right-sided chambers due to tricuspid regurgitation.

underwent a transannular patch type of repair. Some patients also had delayed enhancement in the base of the ventricular septum, corresponding to the site of the ventricular septal defect patch. Harris et al (126) also described delayed enhancement of the RVOT in 31 (91%) of 34 patients who underwent RVOT reconstruction and ventricular septal defect patch closure for correction of conotruncal abnormalities. Delayed enhancement involving the inferior RV insertion point and inferior or lateral LV walls has also been described (127).

The presence of delayed enhancement in RVOT after repair of tetralogy of Fallot has been associated with worse RV function, increased RV volumes and increased RVOT diameter. Interestingly, such an association was not seen in a

Figure 16

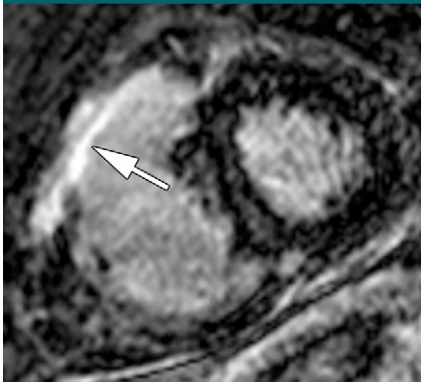


**Figure 16:** Delayed-enhancement inversion-recovery gradient-echo MR image (5/2.3/280) in short-axis plane acquired 15 minutes after injection of a gadolinium chelate in a patient with postoperative tetralogy of Fallot shows extensive delayed enhancement of the RV outflow region (arrow) at site of surgical infundibular myocardial resection.

study involving pediatric patients who underwent repair of conotruncal anomalies (126). The authors of that report suggested that delayed enhancement of the RVOT has a different clinical implication in the adult and pediatric populations. Babu-Narayan et al (127) demonstrated an association between delayed enhancement and adverse clinical markers after tetralogy of Fallot repair, such as ventricular dysfunction, exercise intolerance, and neurohormonal activation. More recently, Wald and co-workers (128) reported a correlation between the extent of delayed enhancement and symptoms of heart failure (New York Heart Association functional class, greater than II) in patients after repair of tetralogy of Fallot.

Delayed enhancement has also been described in the aortic homograft of most patients after Norwood reconstruction for functional single ventricle (126). RV delayed enhancement has been demonstrated in a few patients after repair of transposition of the great arteries, atrial septal defect, and ventricular septal defect (129).

### Future

The report by Kwong et al (63) that a number of patients with known ischemic heart disease but no history of

myocardial infarction show delayed enhancement of the myocardium indicates an expanded role for those techniques in ischemic heart disease. Technical developments in high-field-strength MR units may result in better visualization of microinfarcts and, therefore, add information on risk stratification in these patients. Thus, this technique may become essential in risk assessment and, perhaps, in selection of therapeutic options. Delayed enhancement in patients with ischemic heart disease without acute coronary syndrome may be a harbinger of subsequent large infarction and thus a predictor of adverse cardiovascular events.

Delayed-enhancement MR has been used experimentally to guide transcatheter delivery of genes and multipotential cells to the myocardium as a potential therapy for ischemic cardiomyopathy (130–132). Delayed gadolinium enhancement of the infarction site(s) provides a target for the transcatheter injection of a therapeutic solution during LV catheterization. This approach seems attractive for more precise transcatheter delivery of angiogenesis growth factors and multipotential cells to the periphery of a chronic myocardial infarction.

Most research on and clinical applications of delayed-enhancement MR have until now been directed at the identification and quantification of bulk necrosis and/or fibrosis. Recently, a few reports on the use of delayed gadolinium enhancement to recognize and quantify diffuse myocardial fibrosis have been published (133–135). The technique for quantification of diffuse myocardial fibrosis involves the estimation of the distribution volume of gadolinium in the myocardium based on T1 relaxivity of myocardium relative to that of the blood pool over time. Since the extracellular volume of fibrosis is greater than that of normal myocardium, the distribution volume of diffusely fibrotic myocardium is greater than that of normal myocardium. Diffuse myocardial fibrosis has been identified with this technique in cases of heart failure and dilated cardiomyopathy and in adults with congenital heart disease and ventricular dysfunction. This application indicates a further expansion of

the use of delayed-enhancement MR in the future for aid in characterizing the severity and predicting the outcome of diffuse myocardial diseases.

There has been increased interest in assessing delayed enhancement of the myocardium by using multidetector CT (136–140). It should be remembered that MR is substantially more sensitive to contrast differences than are x-ray-based techniques. Further technology developments in dual-energy CT have the potential capability for improving the contrast between normal and abnormal myocardium. It is questionable, however, whether this will ever reach the contrast sensitivity of the multiple MR sequences now available for myocardial tissue characterization. Moreover, special attention to radiation reduction methods will be crucial for development of a comprehensive CT protocol that includes coronary imaging and viability assessment.

**Disclosures of Potential Conflicts of Interest:** K.G.O. No financial activities to disclose. C.B.H. No financial activities to disclose.

### References

- Higgins CB, Hagen PL, Newell JD, Schmidt WS, Haigler FH. Contrast enhancement of myocardial infarction: dependence on necrosis and residual blood flow and the relationship to distribution of scintigraphic imaging agents. *Circulation* 1982;65(4):739–746.
- Siemers PT, Higgins CB, Schmidt W, Ashburn W, Hagan P. Detection, quantitation and contrast enhancement of myocardial infarction utilizing computerized axial tomography: comparison with histochemical staining and <sup>99m</sup>Tc-pyrophosphate imaging. *Investigative Radiology* 1978;13(2):103–109.
- Mattrey RF, Higgins CB. 1982 Memorial Award Paper. Detection of regional myocardial dysfunction during ischemia with computerized tomography: documentation and physiologic basis. *Invest Radiol* 1982;17(4):329–335.
- Doherty PW, Lipton MJ, Berninger WH, Skioldebrand CG, Carlsson E, Redington RW. Detection and quantitation of myocardial infarction in vivo using transmission computed tomography. *Circulation* 1981;63(3):597–606.
- Huber DJ, Lapray JF, Hessel SJ. In vivo evaluation of experimental myocardial infarcts by un gated computed tomography. *AJR Am J Roentgenol* 1981;136(3):469–473.

6. Wesbey G, Higgins CB, Lipton MJ. Enhancement of myocardial infarctions with nuclear magnetic resonance contrast media. *Invest Radiol* 1984;19(4):S150-S151.
7. McNamara MT, Higgins CB, Ehman RL, Revel D, Sievers R, Brasch RC. Acute myocardial ischemia: magnetic resonance contrast enhancement with gadolinium-DTPA. *Radiology* 1984;153(1):157-163.
8. Tscholakoff D, Higgins CB, Sechtem U, McNamara MT. Occlusive and reperfused myocardial infarcts: effect of Gd-DTPA on ECG-gated MR imaging. *Radiology* 1986;160(2):515-519.
9. McNamara MT, Tscholakoff D, Revel D, et al. Differentiation of reversible and irreversible myocardial injury by MR imaging with and without gadolinium-DTPA. *Radiology* 1986;158(3):765-769.
10. Saeed M, Wendland MF, Takehara Y, Higgins CB. Reversible and irreversible injury in the reperfused myocardium: differentiation with contrast material-enhanced MR imaging. *Radiology* 1990;175(3):633-637.
11. Saeed M, Wendland MF, Yu KK, et al. Identification of myocardial reperfusion with echo planar magnetic resonance imaging. Discrimination between occlusive and reperfused infarctions. *Circulation* 1994;90(3):1492-1501.
12. Judd RM, Lugo-Olivieri CH, Arai M, et al. Physiological basis of myocardial contrast enhancement in fast magnetic resonance images of 2-day-old reperfused canine infarcts. *Circulation* 1995;92(7):1902-1910.
13. Kim RJ, Fieno DS, Parrish TB, et al. Relationship of MRI delayed contrast enhancement to irreversible injury, infarct age, and contractile function. *Circulation* 1999;100(19):1992-2002.
14. Saeed M, Bremerich J, Wendland MF, Wyttenbach R, Weinmann HJ, Higgins CB. Reperfused myocardial infarction as seen with use of necrosis-specific versus standard extracellular MR contrast media in rats. *Radiology* 1999;213(1):247-257.
15. Saeed M, Lund G, Wendland MF, Bremerich J, Weinmann H, Higgins CB. Magnetic resonance characterization of the peri-infarction zone of reperfused myocardial infarction with necrosis-specific and extracellular nonspecific contrast media. *Circulation* 2001;103(6):871-876.
16. Saeed M, Wendland MF, Masui T, Higgins CB. Reperfused myocardial infarctions on T1- and susceptibility-enhanced MRI: evidence for loss of compartmentalization of contrast media. *Magn Reson Med* 1994;31(1):31-39.
17. Geschwind JF, Wendland MF, Saeed M, Lauerma K, Derugin N, Higgins CB. AUR Memorial Award. Identification of myocardial cell death in reperfused myocardial injury using dual mechanisms of contrast-enhanced magnetic resonance imaging. *Acad Radiol* 1994;1(4):319-325.
18. Pereira RS, Prato FS, Wisenberg G, Sykes J. The determination of myocardial viability using Gd-DTPA in a canine model of acute myocardial ischemia and reperfusion. *Magn Reson Med* 1996;36(5):684-693.
19. Pereira RS, Prato FS, Sykes J, Wisenberg G. Assessment of myocardial viability using MRI during a constant infusion of Gd-DTPA: further studies at early and late periods of reperfusion. *Magn Reson Med* 1999;42(1):60-68.
20. Marchal G, Ni Y, Herijgers P, et al. Paramagnetic metalloporphyrins: infarct avid contrast agents for diagnosis of acute myocardial infarction by MRI. *Eur Radiol* 1996;6(1):2-8.
21. Choi SI, Jiang CZ, Lim KH, et al. Application of breath-hold T2-weighted, first-pass perfusion and gadolinium-enhanced T1-weighted MR imaging for assessment of myocardial viability in a pig model. *J Magn Reson Imaging* 2000;11(5):476-480.
22. de Roos A, van Rossum AC, van der Wall E, et al. Reperfused and nonreperfused myocardial infarction: diagnostic potential of Gd-DTPA-enhanced MR imaging. *Radiology* 1989;172(3):717-720.
23. Eichstaedt HW, Felix R, Dougherty FC, Langer M, Rutsch W, Schmutzler H. Magnetic resonance imaging (MRI) in different stages of myocardial infarction using the contrast agent gadolinium-DTPA. *Clin Cardiol* 1986;9(11):527-535.
24. Simonetti OP, Kim RJ, Fieno DS, et al. An improved MR imaging technique for the visualization of myocardial infarction. *Radiology* 2001;218(1):215-223.
25. Wendland MF, Saeed M, Arheden H, et al. Toward necrotic cell fraction measurement by contrast-enhanced MRI of reperfused ischemically injured myocardium. *Acad Radiol* 1998;5(Suppl 1):S42-S44; discussion S45-S46.
26. Arheden H, Saeed M, Higgins CB, et al. Reperfused rat myocardium subjected to various durations of ischemia: estimation of the distribution volume of contrast material with echo-planar MR imaging. *Radiology* 2000;215(2):520-528.
27. Arheden H, Saeed M, Higgins CB, et al. Measurement of the distribution volume of gadopentetate dimeglumine at echo-planar MR imaging to quantify myocardial infarction: comparison with <sup>99m</sup>Tc-DTPA autoradiography in rats. *Radiology* 1999;211(3):698-708.
28. O'Regan DP, Ahmed R, Neuwirth C, et al. Cardiac MRI of myocardial salvage at the peri-infarct border zones after primary coronary intervention. *Am J Physiol Heart Circ Physiol* 2009;297(1):H340-H346.
29. Yan AT, Shayne AJ, Brown KA, et al. Characterization of the peri-infarct zone by contrast-enhanced cardiac magnetic resonance imaging is a powerful predictor of post-myocardial infarction mortality. *Circulation* 2006;114(1):32-39.
30. Azevedo C, Lima JA, Bluemke DA, et al. Tissue heterogeneity by contrast-enhanced MRI as a marker of risk for sudden cardiac death in ischemic cardiomyopathy [abstr]. *Circulation* 2004;110(Suppl III):III-645.
31. de Bakker JM, van Capelle FJ, Janse MJ, et al. Reentry as a cause of ventricular tachycardia in patients with chronic ischemic heart disease: electrophysiologic and anatomic correlation. *Circulation* 1988;77(3):589-606.
32. de Bakker JM, Coronel R, Tasseron S, et al. Ventricular tachycardia in the infarcted, Langendorff-perfused human heart: role of the arrangement of surviving cardiac fibers. *J Am Coll Cardiol* 1990;15(7):1594-1607.
33. Verma A, Marrouche NE, Schweikert RA, et al. Relationship between successful ablation sites and the scar border zone defined by substrate mapping for ventricular tachycardia post-myocardial infarction. *J Cardiovasc Electrophysiol* 2005;16(5):465-471.
34. Pislaru SV, Ni Y, Pislaru C, et al. Noninvasive measurements of infarct size after thrombolysis with a necrosis-avid MRI contrast agent. *Circulation* 1999;99(5):690-696.
35. Lim TH, Choi SI. MRI of myocardial infarction. *J Magn Reson Imaging* 1999;10(5):686-693.
36. Aletras AH, Tilak GS, Natanzon A, et al. Retrospective determination of the area at risk for reperfused acute myocardial infarction with T2-weighted cardiac magnetic resonance imaging: histopathological and displacement encoding with stimulated echoes (DENSE) functional validations. *Circulation* 2006;113(15):1865-1870.
37. Saeed M, Weber O, Lee R, et al. Discrimination of myocardial acute and chronic (scar) infarctions on delayed contrast enhanced magnetic resonance imaging with intravascular magnetic resonance contrast media. *J Am Coll Cardiol* 2006;48(10):1961-1968.
38. Watzinger N, Lund GK, Higgins CB, Chujo M, Saeed M. Noninvasive assessment of the effects of nicorandil on left ventricular volumes and function in reperfused myocardial infarction. *Cardiovasc Res* 2002;54(1):77-84.
39. Saeed M, Watzinger N, Krombach GA, et al. Left ventricular remodeling after

- infarction: sequential MR imaging with oral nicorandil therapy in rat model. *Radiology* 2002;224(3):830-837.
40. Schalla S, Higgins CB, Saeed M. Long-term oral treatment with nicorandil prevents the progression of left ventricular hypertrophy and preserves viability. *J Cardiovasc Pharmacol* 2005;45(4):333-340.
  41. Choi KM, Kim RJ, Gubernikoff G, Vargas JD, Parker M, Judd RM. Transmural extent of acute myocardial infarction predicts long-term improvement in contractile function. *Circulation* 2001;104(10):1101-1107.
  42. Fiengo DS, Kim RJ, Chen EL, Lomasney JW, Klocke FJ, Judd RM. Contrast-enhanced magnetic resonance imaging of myocardium at risk: distinction between reversible and irreversible injury throughout infarct healing. *J Am Coll Cardiol* 2000;36(6):1985-1991.
  43. Lima JA, Judd RM, Bazille A, Schulman SP, Atalar E, Zerhouni EA. Regional heterogeneity of human myocardial infarcts demonstrated by contrast-enhanced MRI. Potential mechanisms. *Circulation* 1995;92(5):1117-1125.
  44. Kim RJ, Wu E, Rafael A, et al. The use of contrast-enhanced magnetic resonance imaging to identify reversible myocardial dysfunction. *N Engl J Med* 2000;343(20):1445-1453.
  45. Rogers WJ Jr, Kramer CM, Geskin G, et al. Early contrast-enhanced MRI predicts late functional recovery after reperfused myocardial infarction. *Circulation* 1999;99(6):744-750.
  46. Kramer CM, Rogers WJ Jr, Mankad S, Theobald TM, Pakstis DL, Hu YL. Contractile reserve and contrast uptake pattern by magnetic resonance imaging and functional recovery after reperfused myocardial infarction. *J Am Coll Cardiol* 2000;36(6):1835-1840.
  47. Ramani K, Judd RM, Holly TA, et al. Contrast magnetic resonance imaging in the assessment of myocardial viability in patients with stable coronary artery disease and left ventricular dysfunction. *Circulation* 1998;98(24):2687-2694.
  48. Ibrahim T, Bülow HP, Hackl T, et al. Diagnostic value of contrast-enhanced magnetic resonance imaging and single-photon emission computed tomography for detection of myocardial necrosis early after acute myocardial infarction. *J Am Coll Cardiol* 2007;49(2):208-216.
  49. Ingkanisorn WP, Rhoads KL, Aletras AH, Kellman P, Arai AE. Gadolinium delayed enhancement cardiovascular magnetic resonance correlates with clinical measures of myocardial infarction. *J Am Coll Cardiol* 2004;43(12):2253-2259.
  50. Bello D, Shah DJ, Farah GM, et al. Gadolinium cardiovascular magnetic resonance predicts reversible myocardial dysfunction and remodeling in patients with heart failure undergoing beta-blocker therapy. *Circulation* 2003;108(16):1945-1953.
  51. Klem I, Heitner JF, Shah DJ, et al. Improved detection of coronary artery disease by stress perfusion cardiovascular magnetic resonance with the use of delayed enhancement infarction imaging. *J Am Coll Cardiol* 2006;47(8):1630-1638.
  52. Ansari M, Araoz PA, Gerard SK, et al. Comparison of late enhancement cardiovascular magnetic resonance and thallium SPECT in patients with coronary disease and left ventricular dysfunction. *J Cardiovasc Magn Reson* 2004;6(2):549-556.
  53. Ichikawa Y, Sakuma H, Suzawa N, et al. Late gadolinium-enhanced magnetic resonance imaging in acute and chronic myocardial infarction. Improved prediction of regional myocardial contraction in the chronic state by measuring thickness of non-enhanced myocardium. *J Am Coll Cardiol* 2005;45(6):901-909.
  54. Kim RJ, Albert TS, Wible JH, et al. Performance of delayed-enhancement magnetic resonance imaging with gadoversetamide contrast for the detection and assessment of myocardial infarction: an international, multicenter, double-blinded, randomized trial. *Circulation* 2008;117(5):629-637.
  55. Wu E, Judd RM, Vargas JD, Klocke FJ, Bonow RO, Kim RJ. Visualisation of presence, location, and transmural extent of healed Q-wave and non-Q-wave myocardial infarction. *Lancet* 2001;357(9249):21-28.
  56. Wagner A, Mahrholdt H, Holly TA, et al. Contrast-enhanced MRI and routine single photon emission computed tomography (SPECT) perfusion imaging for detection of subendocardial myocardial infarcts: an imaging study. *Lancet* 2003;361(9355):374-379.
  57. Moon JC, De Arenaza DP, Elkington AG, et al. The pathologic basis of Q-wave and non-Q-wave myocardial infarction: a cardiovascular magnetic resonance study. *J Am Coll Cardiol* 2004;44(3):554-560.
  58. Schulz-Menger J, Gross M, Messroghli D, Uhlich F, Dietz R, Friedrich MG. Cardiovascular magnetic resonance of acute myocardial infarction at a very early stage. *J Am Coll Cardiol* 2003;42(3):513-518.
  59. Wellnhofer E, Olariu A, Klein C, et al. Magnetic resonance low-dose dobutamine test is superior to SCAR quantification for the prediction of functional recovery. *Circulation* 2004;109(18):2172-2174.
  60. Klein C, Nekolla SG, Bengel FM, et al. Assessment of myocardial viability with contrast-enhanced magnetic resonance imaging: comparison with positron emission tomography. *Circulation* 2002;105(2):162-167.
  61. Knuesel PR, Nanz D, Wyss C, et al. Characterization of dysfunctional myocardium by positron emission tomography and magnetic resonance: relation to functional outcome after revascularization. *Circulation* 2003;108(9):1095-1100.
  62. Nelson C, McCrohon J, Khafagi F, Rose S, Leano R, Marwick TH. Impact of scar thickness on the assessment of viability using dobutamine echocardiography and thallium single-photon emission computed tomography: a comparison with contrast-enhanced magnetic resonance imaging. *J Am Coll Cardiol* 2004;43(7):1248-1256.
  63. Kwong RY, Chan AK, Brown KA, et al. Impact of unrecognized myocardial scar detected by cardiac magnetic resonance imaging on event-free survival in patients presenting with signs or symptoms of coronary artery disease. *Circulation* 2006;113(23):2733-2743.
  64. Barbier CE, Bjerner T, Johansson L, Lind L, Ahlström H. Myocardial scars more frequent than expected: magnetic resonance imaging detects potential risk group. *J Am Coll Cardiol* 2006;48(4):765-771.
  65. Wu KC, Kim RJ, Bluemke DA, et al. Quantification and time course of microvascular obstruction by contrast-enhanced echocardiography and magnetic resonance imaging following acute myocardial infarction and reperfusion. *J Am Coll Cardiol* 1998;32(6):1756-1764.
  66. Wu KC, Zerhouni EA, Judd RM, et al. Prognostic significance of microvascular obstruction by magnetic resonance imaging in patients with acute myocardial infarction. *Circulation* 1998;97(8):765-772.
  67. Gerber BL, Rochitte CE, Melin JA, et al. Microvascular obstruction and left ventricular remodeling early after acute myocardial infarction. *Circulation* 2000;101(23):2734-2741.
  68. Nijveldt R, Beek AM, Hofman MB, et al. Late gadolinium-enhanced cardiovascular magnetic resonance evaluation of infarct size and microvascular obstruction in optimally treated patients after acute myocardial infarction. *J Cardiovasc Magn Reson* 2007;9(5):765-770.
  69. Bogaert J, Kalantzi M, Rademakers FE, Dymarkowski S, Janssens S. Determinants and impact of microvascular obstruction in successfully reperfused ST-segment elevation myocardial infarction. Assessment by magnetic resonance imaging. *Eur Radiol* 2007;17(10):2572-2580.

70. Bello D, Fieno DS, Kim RJ, et al. Infarct morphology identifies patients with substrate for sustained ventricular tachycardia. *J Am Coll Cardiol* 2005;45(7):1104–1108.
71. Schmidt A, Azevedo CF, Cheng A, et al. Infarct tissue heterogeneity by magnetic resonance imaging identifies enhanced cardiac arrhythmia susceptibility in patients with left ventricular dysfunction. *Circulation* 2007;115(15):2006–2014.
72. Mahrholdt H, Goedecke C, Wagner A, et al. Cardiovascular magnetic resonance assessment of human myocarditis: a comparison to histology and molecular pathology. *Circulation* 2004;109(10):1250–1258.
73. Mahrholdt H, Wagner A, Deluigi CC, et al. Presentation, patterns of myocardial damage, and clinical course of viral myocarditis. *Circulation* 2006;114(15):1581–1590.
74. Abdel-Aty H, Boyé P, Zagrosek A, et al. Diagnostic performance of cardiovascular magnetic resonance in patients with suspected acute myocarditis: comparison of different approaches. *J Am Coll Cardiol* 2005;45(11):1815–1822.
75. Laissy JP, Hyafil F, Feldman LJ, et al. Differentiating acute myocardial infarction from myocarditis: diagnostic value of early- and delayed-perfusion cardiac MR imaging. *Radiology* 2005;237(1):75–82.
76. Ingkanisorn WP, Paterson DI, Calvo KR, et al. Cardiac magnetic resonance appearance of myocarditis caused by high dose IL-2: similarities to community-acquired myocarditis. *J Cardiovasc Magn Reson* 2006;8(2):353–360.
77. Gutberlet M, Spors B, Thoma T, et al. Suspected chronic myocarditis at cardiac MR: diagnostic accuracy and association with immunohistologically detected inflammation and viral persistence. *Radiology* 2008;246(2):401–409.
78. De Cobelli F, Pieroni M, Esposito A, et al. Delayed gadolinium-enhanced cardiac magnetic resonance in patients with chronic myocarditis presenting with heart failure or recurrent arrhythmias. *J Am Coll Cardiol* 2006;47(8):1649–1654.
79. Yilmaz A, Mahrholdt H, Athanasiadis A, et al. Coronary vasospasm as the underlying cause for chest pain in patients with PVB19 myocarditis. *Heart* 2008;94(11):1456–1463.
80. Wagner A, Schulz-Menger J, Dietz R, Friedrich MG. Long-term follow-up of patients paragon sign with acute myocarditis by magnetic resonance imaging. *MAGMA* 2003;16(1):17–20.
81. McCrohon JA, Moon JC, Prasad SK, et al. Differentiation of heart failure related to dilated cardiomyopathy and coronary artery disease using gadolinium-enhanced cardiovascular magnetic resonance. *Circulation* 2003;108(1):54–59.
82. Tigen K, Karaahmet T, Kirma C, et al. Diffuse late gadolinium enhancement by cardiovascular magnetic resonance predicts significant intraventricular systolic dyssynchrony in patients with non-ischemic dilated cardiomyopathy. *J Am Soc Echocardiogr* 2010;23(4):416–422.
83. Choudhury L, Mahrholdt H, Wagner A, et al. Myocardial scarring in asymptomatic or mildly symptomatic patients with hypertrophic cardiomyopathy. *J Am Coll Cardiol* 2002;40(12):2156–2164.
84. Kim RJ, Judd RM. Gadolinium-enhanced magnetic resonance imaging in hypertrophic cardiomyopathy: in vivo imaging of the pathologic substrate for premature cardiac death? *J Am Coll Cardiol* 2003;41(9):1568–1572.
85. Moon JC, Reed E, Sheppard MN, et al. The histologic basis of late gadolinium enhancement cardiovascular magnetic resonance in hypertrophic cardiomyopathy. *J Am Coll Cardiol* 2004;43(12):2260–2264.
86. Kuribayashi T, Roberts WC. Myocardial disarray at junction of ventricular septum and left and right ventricular free walls in hypertrophic cardiomyopathy. *Am J Cardiol* 1992;70(15):1333–1340.
87. Basso C, Thiene G, Corrado D, Buja G, Melacini P, Nava A. Hypertrophic cardiomyopathy and sudden death in the young: pathologic evidence of myocardial ischemia. *Hum Pathol* 2000;31(8):988–998.
88. Shirani J, Pick R, Roberts WC, Maron BJ. Morphology and significance of the left ventricular collagen network in young patients with hypertrophic cardiomyopathy and sudden cardiac death. *J Am Coll Cardiol* 2000;35(1):36–44.
89. Varnava AM, Elliott PM, Baboonian C, Davison F, Davies MJ, McKenna WJ. Hypertrophic cardiomyopathy: histopathological features of sudden death in cardiac troponin T disease. *Circulation* 2001;104(12):1380–1384.
90. Adabag AS, Maron BJ, Appelbaum E, et al. Occurrence and frequency of arrhythmias in hypertrophic cardiomyopathy in relation to delayed enhancement on cardiovascular magnetic resonance. *J Am Coll Cardiol* 2008;51(14):1369–1374.
91. Satoh H, Matoh F, Shiraki K, et al. Delayed enhancement on cardiac magnetic resonance and clinical, morphological, and electrocardiographical features in hypertrophic cardiomyopathy. *J Card Fail* 2009;15(5):419–427.
92. Moon JC, McKenna WJ, McCrohon JA, Elliott PM, Smith GC, Pennell DJ. Toward clinical risk assessment in hypertrophic cardiomyopathy with gadolinium cardiovascular magnetic resonance. *J Am Coll Cardiol* 2003;41(9):1561–1567.
93. Shammam RL, Movahed A. Sarcoidosis of the heart. *Clin Cardiol* 1993;16(6):462–472.
94. Silverman KJ, Hutchins GM, Bulkley BH. Cardiac sarcoid: a clinicopathologic study of 84 unselected patients with systemic sarcoidosis. *Circulation* 1978;58(6):1204–1211.
95. Roberts WC, McAllister HA Jr, Ferrans VJ. Sarcoidosis of the heart. A clinicopathologic study of 35 necropsy patients (group I) and review of 78 previously described necropsy patients (group II). *Am J Med* 1977;63(1):86–108.
96. Vignaux O. Cardiac sarcoidosis: spectrum of MRI features. *AJR Am J Roentgenol* 2005;184(1):249–254.
97. Ichinose A, Otani H, Oikawa M, et al. MRI of cardiac sarcoidosis: basal and subepicardial localization of myocardial lesions and their effect on left ventricular function. *AJR Am J Roentgenol* 2008;191(3):862–869.
98. Patel MR, Cawley PJ, Heitner JF, et al. Detection of myocardial damage in patients with sarcoidosis. *Circulation* 2009;120(20):1969–1977.
99. Smedema JP, Snoep G, van Kroonenburgh MP, et al. Cardiac involvement in patients with pulmonary sarcoidosis assessed at two university medical centers in the Netherlands. *Chest* 2005;128(1):30–35.
100. Matoh F, Satoh H, Shiraki K, et al. The usefulness of delayed enhancement magnetic resonance imaging for diagnosis and evaluation of cardiac function in patients with cardiac sarcoidosis. *J Cardiol* 2008;51(3):179–188.
101. Smedema JP, Snoep G, van Kroonenburgh MP, et al. The additional value of gadolinium-enhanced MRI to standard assessment for cardiac involvement in patients with pulmonary sarcoidosis. *Chest* 2005;128(3):1629–1637.
102. Vogelsberg H, Mahrholdt H, Deluigi CC, et al. Cardiovascular magnetic resonance in clinically suspected cardiac amyloidosis: noninvasive imaging compared to endomyocardial biopsy. *J Am Coll Cardiol* 2008;51(10):1022–1030.
103. Maceira AM, Joshi J, Prasad SK, et al. Cardiovascular magnetic resonance in cardiac amyloidosis. *Circulation* 2005;111(2):186–193.
104. Perugini E, Rapezzi C, Piva T, et al. Noninvasive evaluation of the myocardial substrate of cardiac amyloidosis by gadolinium cardiac magnetic resonance. *Heart* 2006;92(3):343–349.

105. Mahrholdt H, Wagner A, Judd RM, Sechtem U, Kim RJ. Delayed enhancement cardiovascular magnetic resonance assessment of non-ischaemic cardiomyopathies. *Eur Heart J* 2005;26(15):1461–1474.
106. Hosch W, Kristen AV, Libicher M, et al. Late enhancement in cardiac amyloidosis: correlation of MRI enhancement pattern with histopathological findings. *Amyloid* 2008;15(3):196–204.
107. Becker AE, Anderson HR. Cardiac pathology. New York, NY: Raven, 1983.
108. Ruberg FL, Appelbaum E, Davidoff R, et al. Diagnostic and prognostic utility of cardiovascular magnetic resonance imaging in light-chain cardiac amyloidosis. *Am J Cardiol* 2009;103(4):544–549.
109. Pfluger HB, Phrommintikul A, Mariani JA, Cherayath JG, Taylor AJ. Utility of myocardial fibrosis and fatty infiltration detected by cardiac magnetic resonance imaging in the diagnosis of arrhythmogenic right ventricular dysplasia—a single centre experience. *Heart Lung Circ* 2008;17(6):478–483.
110. Tandri H, Saranathan M, Rodriguez ER, et al. Noninvasive detection of myocardial fibrosis in arrhythmogenic right ventricular cardiomyopathy using delayed-enhancement magnetic resonance imaging. *J Am Coll Cardiol* 2005;45(1):98–103.
111. De Cobelli F, Esposito A, Belloni E, et al. Delayed-enhanced cardiac MRI for differentiation of Fabry's disease from symmetric hypertrophic cardiomyopathy. *AJR Am J Roentgenol* 2009;192(3):W97–W102.
112. Rochitte CE, Oliveira PF, Andrade JM, et al. Myocardial delayed enhancement by magnetic resonance imaging in patients with Chagas' disease: a marker of disease severity. *J Am Coll Cardiol* 2005;46(8):1553–1558.
113. Rochitte CE, Nacif MS, de Oliveira Júnior AC, et al. Cardiac magnetic resonance in Chagas' disease. *Artif Organs* 2007;31(4):259–267.
114. Baccouche H, Yilmaz A, Alscher D, Klingel K, Val-Bernal JF, Mahrholdt H. Images in cardiovascular medicine. Magnetic resonance assessment and therapy monitoring of cardiac involvement in Churg-Strauss syndrome. *Circulation* 2008;117(13):1745–1749.
115. Chun W, Grist TM, Kamp TJ, Warner TF, Christian TF. Images in cardiovascular medicine. Infiltrative eosinophilic myocarditis diagnosed and localized by cardiac magnetic resonance imaging. *Circulation* 2004;110(3):e19.
116. Petersen SE, Kardos A, Neubauer S. Subendocardial and papillary muscle involvement in a patient with Churg-Strauss syndrome, detected by contrast enhanced cardiovascular magnetic resonance. *Heart* 2005;91(1):e9.
117. Lelovas P, Dontas I, Bassiakou E, Xanthos T. Cardiac implications of Lyme disease, diagnosis and therapeutic approach. *Int J Cardiol* 2008;129(1):15–21.
118. Naik M, Kim D, O'Brien F, Axel L, Srichai MB. Images in cardiovascular medicine. Lyme carditis. *Circulation* 2008;118(18):1881–1884.
119. Karadag B, Spieker LE, Schwitter J, et al. Lyme carditis: restitutio ad integrum documented by cardiac magnetic resonance imaging. *Cardiol Rev* 2004;12(4):185–187.
120. Paydar A, Ordovas KG, Reddy GP. Magnetic resonance imaging for endomyocardial fibrosis. *Pediatr Cardiol* 2008;29(5):1004–1005.
121. Salantri GC. Endomyocardial fibrosis and intracardiac thrombus occurring in idiopathic hypereosinophilic syndrome. *AJR Am J Roentgenol* 2005;184(5):1432–1433.
122. Chao BH, Cline-Parhamovich K, Grizzard JD, Smith TJ. Fatal Loeffler's endocarditis due to hypereosinophilic syndrome. *Am J Hematol* 2007;82(10):920–923.
123. Plastiras SC, Economopoulos N, Kelekis NL, Tzelepis GE. Magnetic resonance imaging of the heart in a patient with hypereosinophilic syndrome. *Am J Med* 2006;119(2):130–132.
124. Syed IS, Martinez MW, Feng DL, Glockner JF. Cardiac magnetic resonance imaging of eosinophilic endomyocardial disease. *Int J Cardiol* 2008;126(3):e50–e52.
125. Oosterhof T, Mulder BJ, Vliegen HW, de Roos A. Corrected tetralogy of Fallot: delayed enhancement in right ventricular outflow tract. *Radiology* 2005;237(3):868–871.
126. Harris MA, Johnson TR, Weinberg PM, Fogel MA. Delayed-enhancement cardiovascular magnetic resonance identifies fibrous tissue in children after surgery for congenital heart disease. *J Thorac Cardiovasc Surg* 2007;133(3):676–681.
127. Babu-Narayan SV, Kilner PJ, Li W, et al. Ventricular fibrosis suggested by cardiovascular magnetic resonance in adults with repaired tetralogy of Fallot and its relationship to adverse markers of clinical outcome. *Circulation* 2006;113(3):405–413.
128. Wald RM, Haber I, Wald R, Valente AM, Powell AJ, Geva T. Effects of regional dysfunction and late gadolinium enhancement on global right ventricular function and exercise capacity in patients with repaired tetralogy of Fallot. *Circulation* 2009;119(10):1370–1377.
129. Hartke LP, Gilkeson RC, O'Riordan MA, Siwik ES. Evaluation of right ventricular fibrosis in adult congenital heart disease using gadolinium-enhanced magnetic resonance imaging: initial experience in patients with right ventricular loading conditions. *Congenit Heart Dis* 2006;1(5):192–201.
130. Kraitchman DL, Heldman AW, Atalar E, et al. In vivo magnetic resonance imaging of mesenchymal stem cells in myocardial infarction. *Circulation* 2003;107(18):2290–2293.
131. Dick AJ, Guttman MA, Raman VK, et al. Magnetic resonance fluoroscopy allows targeted delivery of mesenchymal stem cells to infarct borders in Swine. *Circulation* 2003;108(23):2899–2904.
132. Saeed M, Martin AJ, Lee RJ, et al. MR guidance of targeted injections into border and core of scarred myocardium in pigs. *Radiology* 2006;240(2):419–426.
133. Iles L, Pfluger H, Phrommintikul A, et al. Evaluation of diffuse myocardial fibrosis in heart failure with cardiac magnetic resonance contrast-enhanced T1 mapping. *J Am Coll Cardiol* 2008;52(19):1574–1580.
134. Pack NA, Dibella EV, Wilson BD, McGann CJ. Quantitative myocardial distribution volume from dynamic contrast-enhanced MRI. *Magn Reson Imaging* 2008;26(4):532–542.
135. Jerosch-Herold M, Sheridan DC, Kushner JD, et al. Cardiac magnetic resonance imaging of myocardial contrast uptake and blood flow in patients affected with idiopathic or familial dilated cardiomyopathy. *Am J Physiol Heart Circ Physiol* 2008;295(3):H1234–H1242.
136. Gerber B. Comprehensive cardiac imaging using multidetector CT and magnetic resonance imaging [in French]. *Bull Mem Acad R Med Belg* 2009;164(3-4):103–107; discussion 107–108.
137. Blankstein R, Rogers IS, Cury RC. Practical tips and tricks in cardiovascular computed tomography: diagnosis of myocardial infarction. *J Cardiovasc Comput Tomogr* 2009;3(2):104–111.
138. Krombach GA, Niendorf T, Günther RW, Mahnken AH. Characterization of myocardial viability using MR and CT imaging. *Eur Radiol* 2007;17(6):1433–1444.
139. Bousset L, Ribagnac M, Bonnefoy E, et al. Assessment of acute myocardial infarction using MDCT after percutaneous coronary intervention: comparison with MRI. *AJR Am J Roentgenol* 2008;191(2):441–447.
140. Furtado AD, Carlsson M, Wintermark M, Ordovas K, Saeed M. Identification of residual ischemia, infarction, and microvascular impairment in revascularized myocardial infarction using 64-slice MDCT. *Contrast Media Mol Imaging* 2008;3(5):198–206.